Ultrafast all-optical modulation in GaAs photonic crystal cavities

Chad Husko, ^{1,a)} Alfredo De Rossi, ^{1,b)} Sylvain Combrié, ¹ Quynh Vy Tran, ¹ Fabrice Raineri, ^{2,c)} and Chee Wei Wong ³

(Received 4 November 2008; accepted 19 December 2008; published online 14 January 2009)

We demonstrate all-optical modulation based on ultrafast optical carrier injection in a GaAs photonic crystal cavity using a degenerate pump-probe technique. The observations agree well with a coupled-mode model incorporating all relevant nonlinearities. The low switching energy (\sim 120 fJ), small energy absorption (\sim 10 fJ), fast on-off response (\sim 15 ps), limited only by carrier lifetime, and a minimum 10 dB modulation depth suggest practical all-optical switching applications at high repetition rates. © 2009 American Institute of Physics.

[DOI: 10.1063/1.3068755]

On-chip all-optical semiconductor switching has attracted a significant amount of attention in recent years. Various approaches to high-speed devices have been investigated involving the plasma dispersion effect in silicon photonic crystal (PhC) cavities and optically pumped silicon microrings.² The free carriers that cause the plasma effect and consequent refractive index shift are generated from two-photon absorption (TPA). All-optical modulation has also been achieved in III-V microrings.3 In each of these experiments, the fundamental limit of the switching speed is the effective carrier lifetime $au_{\rm eff}$. Advanced semiconductor processing techniques such as ion implantation 4 and p-i-ndiodes² have reduced $\tau_{\rm eff}$ to 70 and 50 ps, respectively, in crystalline silicon, though at the cost of increased optical loss or power threshold. Designs incorporating two-color switching mechanisms have achieved faster speeds than their single color counterparts but have decidedly more challenging fabrication processing involving the following: (a) selective area growth of highly homogeneous self-assembled quantum dots⁵ (2 ps), (b) three-dimensional polysilicon PhCs (Ref. 6) (18 ps), or (c) a silicon and Kerr-polymer hybrid waveguide (WG) Mach-Zender⁷ (10 GHz). Despite the variety of approaches, due to their ability to strongly confine light, 8,9 reduced $\tau_{\rm eff}$, and enhanced light-matter interaction, $^{10-12}$ we believe PhC cavities are the most promising approach for achieving high-speed, low-power, switches and memory. In this letter, we demonstrate a single color, ultrafast nonlinear response due to the plasma dispersion effect in a GaAs PhC cavity with a recovery time less than 10 ps.

An approach for an all-optical switch is to modulate the refractive index of the material. Instead of near-instantaneous all-optical Kerr, we suggest that an efficient TPA induced plasma effect coupled with fast carrier recovery is also a viable option. ¹³ In this respect, we performed degenerate pump-probe experiments on PhC cavities fabricated in GaAs, a material known for its large TPA coefficient β and elevated electron mobility. The combination of high mobility

The PhC structure studied here is an in-line, overcoupled H0 cavity in an air slab structure with a thickness of 250 nm based on a triangular lattice (period a=430 nm) of holes with radius r=0.22a. We used the design proposed in Ref. 14 providing ultrasmall mode volume of $0.24(\lambda/n)^3$. The cavity is formed from two air holes shifted by s=0.16a three rows above the WG. The holes nearest the PhC WG are enlarged to $r_{wg} = 0.34a$ in order to couple light to the cavity mode. All quoted distances are nominal. The fabrication process and the detailed linear characterization of similar structures have been described elsewhere. 17 The cavity resonant wavelength is measured to be 1540.05 nm with a full width at half maximum (FWHM) of 1.2 nm, as shown in Fig. 1. The coupling loss into the WG, here \sim -5 dB/facet, is estimated after accounting for the losses due to the microscope objectives, as well as the mode adaptation of the free-space beam coupled into the PhC. 13 The small insertion loss here is due to a mode adapter, the details of which will be published elsewhere. The linear transmission of the PhC sample was therefore estimated to be 90% with the cavity on-resonance. The FWHM and transmission data yield loaded and intrinsic Q-factors of $Q_L = \lambda_0 / \Delta \lambda = 1$, 200 and $Q_i = 2.5 \times 10^4$, respectively. ¹⁸ The cavity photon lifetime is $\tau_{\rm ph} = Q_L \lambda_0 / 2\pi c$ ≈ 1 ps, thereby intentionally ensuring that the switching

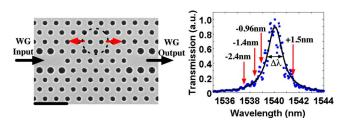


FIG. 1. (Color online) Left: SEM of cavity region. The innermost holes were shifted s=0.16a. Scale bar: 1 μ m. Right: Cavity resonance with arrows indicating various detuning regions where pump-probe measurements were carried out.

¹Thales Research and Technology, Route Départementale 128, 91767 Palaiseau, France

²Laboratoire de Photonique et de Nanostructures (CNRS UPR 20), Route de Nozay, 91460 Marcoussis, France

³Optical Nanostructures Laboratory, Columbia University, New York, New York 10027 USA

and enhanced surface to volume ratio S/V of the GaAs PhC nanocavity greatly reduce $\tau_{\rm eff}$, reaching values as low as 8 ps in AlGaAs PhC lattices without resonant cavities. An additional advantage of GaAs is the ability to embed active materials, such as quantum wells or dots. 5,15,16

a)Electronic mail: cah2116@columbia.edu. Also at Columbia University, New York, U.S.A.

b) Electronic mail: alfredo.derossi@thalesgroup.com.

c) Also at Université D. Diderot, 75205 Paris, France.

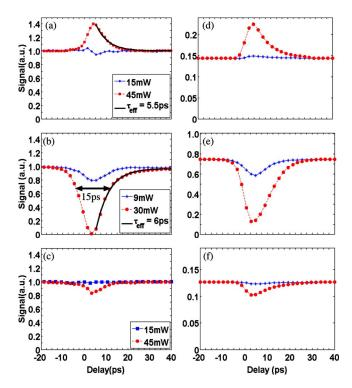


FIG. 2. (Color online) Experiment [(a)–(c)] and CMT [(d)–(f)] pump-probe transmission data. The plots correspond to different detunings as outlined in Fig. 1. Quoted values are peak power. (a) $\Delta\lambda$ =-1.4 nm, (b) $\Delta\lambda$ =0, and (c) $\Delta\lambda$ =+1.5 nm. The solid black lines in (a) and (b) are the fits for the carrier recombination lifetimes. [(d)–(f)] CMT: Respective detunings with simulated pump powers 9 and 30 mW.

speed was not limited by the cavity photon lifetime and allowed us to focus on the intrinsic material free carrier lifetime.

For the nonlinear measurements, we employ a degenerate pump-probe technique in order to observe the dynamics of the GaAs PhC cavity system. A wavelength tunable modelocked fiber laser (PriTel) with 3.5–4 ps pulses at a repetition rate of 22 MHz with the polarization set to transverse electric (TE), or electric field in the plane of the PC slab, was employed to investigate the nonlinear properties of the sample. The pulse behavior is monitored with an optical spectrum analyzer and an oscilloscope. The beam is split into pump and probe branches with a mechanical chopper (400 Hz) placed in the attenuated probe branch to distinguish between the two beams. 19 After recombining with the pump branch, the signal is coupled to the PhC WG through microscope objectives (Zeiss, numerical aperture 0.95). The transmitted signal is detected with a photodiode, amplified, and monitored with a lock-in amplifier. We define a positive delay as the pump arriving before the probe and the detuning as $\Delta\lambda$ $=\lambda_{laser}-\lambda_0$. We verified that the probe was sufficiently weak so as to remain in the linear regime, i.e., it did not cause any nonlinear effects in the sample.

Figure 2 shows two of the cases for which we varied the detuning and pump power. After accounting for the insertion loss at the entry facet and assuming negligible loss in the PhC WG,²⁰ we estimate the pulse energies in the cavity for a 30 mW peak power to be 120 fJ. Since the spectral width of the cavity (1.2 nm) exceeds that of the pulse $\sim 0.7 \text{ nm}$, the input beam is entirely within the cavity bandwidth and thus we assume that all of the pulse energy enters the cavity. Peak

powers were varied from 9 to 66 mW. Quoted power levels are the power coupled into the WG.

For the on-resonance case, Fig. 2(b), an input pulse with 30 mW peak power shifts the cavity resonance such that the transmission approaches zero. Increasing pump power further saturates the curve. We estimate an index shift $\Delta n = n\Delta \lambda/\lambda = 2.6 \times 10^{-3}$ per previous studies in III-V materials. The resonance shift allows for a minimum modulation depth of 10 dB, though we expect the actual value to be much larger.

We then blue detune the laser to $\Delta \lambda = -1.4$ nm. The results are plotted in Fig. 2(a). At a low input peak power of 15 mW, the curve remains largely flat as the powers are too small to cause a nonlinear effect. At an increased pump power of 45 mW, the transmission curve demonstrates a sharp upward peak, which has several implications. First, this peak corresponds to increased transmission due to the plasma dispersion effect which initiates a blue shift in the cavity resonance λ_0 to reach the laser frequency λ_{laser} . In the in-line geometry, the cavity now has increased transmission. Second, the upward peak is direct proof that the plasma effect is the dominant effect at this picosecond timescale.²¹ Finally, and most importantly, the presence of a peak, in lieu of a dip, at increased pump powers demonstrates that TPA effects are minimal. This is a clear demonstration of efficient nonlinear effects in GaAs PhC cavities. One can clearly see the asymmetric peak with the free-carrier effect at a positive delay. A fit of the experimental data in Fig. 2(a) (solid black line) suggests a 1/e recovery time of ~ 6 ps for the system. We also fit Fig. 2(b) and found a similar result. The total rise and fall time is approximately 15 ps. We further conducted measurements at a far detuning of -2.4 nm (not pictured here). The largest pump power of 66 mW reported here results in a flat transmission plot, indicating that the pump beam cannot sufficiently couple to the cavity resonance and initiate a feedback loop that is characteristic of nonlinear cavities. 10

As we move to a positive detuning, Fig. 2(c), the roles of the competing thermal and free-carrier effects are modified. At a red detuning of $\Delta\lambda$ =+1.5 nm, the fast plasma effect pushes the resonance to lower wavelengths, reducing the transmission. The repetition rates employed here ensure that a slow thermal effect (microsecond) cannot build up in time. As we increase to larger positive detunings (not pictured here), the contrast for a given pump power in fact decreases due to the smaller amount of energy coupled into the cavity and consequently smaller nonlinear cavity resonance shift.

We employed coupled-mode theory (CMT) to confirm the behavior of the PhC cavity as in our previous work. Simulations were carried out with parameters calculated (e.g., the mode and nonlinear volumes) or known in the literature. The results are plotted in Figs. 2(d)–2(f). Importantly, the modeled input peak powers are on the same order of magnitude as the experiments. The experimental values above are assumed to be an upper bound. It is expected that some portion will be lost to cavity coupling at different detunings and linear loss. We thus fix the peak powers to 9 and 30 mW for the low and high power cases, respectively, in the simulation.

Let us now compare those values with the literature by introducing the appropriate scaling for resonant switching based on TPA and carrier plasma. The peak power required for switching is $P_{\rm sw} \propto V_{\rm cavity}/Q^2$, where $V_{\rm cavity}$ is the cavity

FIG. 3. (Color online) CMT (a) Cavity response for on-resonance case. Left axis: Instantaneous cavity power (milliwatt) Right axis: Instantaneous absorbed power (milliwatt) (b) Carrier concentration in the cavity (cm⁻³).

volume. Interestingly this is the same as for Kerr-based switching. Thus, the energy per pulse required for switching is $W_{\text{switch}} \propto V_{\text{cavity}} \Delta \nu_c \beta_2^{-1/2}$ for a given bandwidth $\Delta \nu_c$. A faster response time implies using more energy per pulse. We improved the dynamic response by an order of magnitude with just a twofold increase in energy per pulse. This remarkable result is due to the ultrasmall mode volume of the cavity and the tenfold larger TPA coefficient of GaAs as compared to silicon. The CMT confirms that the energy absorbed by TPA is 10 fJ (\sim 8%), which is comparable to the best currently reported values in silicon PhC cavities. 4 The instantaneous cavity power and absorbed power are plotted in Fig. 3(a). The coupled-mode model predicts a peak carrier concentration of 2×10^{17} cm⁻³ under these conditions, as shown in Fig. 3(b). We conclude that the plasma effect is the dominant effect in achieving in the modulation.

In conclusion, we have demonstrated an ultrafast and low power (120 fJ pulse energy) all-optical modulation based on TPA and carrier plasma frequency shift implemented with a resonant ultrasmall PhC cavity made of GaAs. We achieved a 10 dB extinction ratio with moderate peak powers (30–45 mW), available from current telecom laser diode technology. The ultrafast response is due to the extremely short effective carrier lifetime in GaAs and the high surface to volume ratio typical of nanostructures such as PhCs. Using the experimental values, we modeled the behavior of the pump beam at a repetition rate of 40 Gb/s per channel, and observed a 10 dB transmission contrast that compared well with the experimentally demonstrated values at 22 MHz. The quick recovery of the system, as well as the very small en-

ergy budget per switching operation, make GaAs PhC cavities strong candidates for future all-optical networks.

One of the authors (C.H.) thanks the Fulbright Grant for financial support.

¹T. Tanabe, M. Notomi, S. Mitsugi, A. Shinya, and E. Kuramochi, Opt. Lett. **30**, 2575 (2005).

²S. Preble, Q. Xu, B. Schmidt, and M. Lipson, Opt. Lett. **30**, 2891 (2005).

³V. Van, T. A. Ibrahim, K. Ritter, P. P. Absil, F. G. Johnson, R. Grover, J.

Goldhar, and P.-T. Ho, IEEE Photon. Technol. Lett. **14**, 74 (2002). ⁴T. Tanabe, K. Nishiguchi, A. Shinya, E. Kuramochi, H. Inokawa, M. Notomi, K. Yamada, T. Tsuchizawa, T. Watanabe, H. Fukuda, H. Shinojima, and H. Itabashi, Appl. Phys. Lett. **90**, 031115 (2007).

⁵H. Nakamura, Y. Sugimoto, K. Kanamoto, N. Ikeda, Y. Tanaka, Y. Nakamura, S. Ohkouchi, Y. Watanabe, K. Inoue, H. Ishikawa, and K. Asakawa, Opt. Express 12, 6606 (2004).

⁶T. Euser, A. Molenaar, J. Fleming, B. Gralak, A. Polman, and W. Vos, Phys. Rev. B 77, 115214 (2008).

⁷M. Hochberg, T. Baehr-Jones, G. Wang, M. Shearn, K. Harvard, J. Luo, B. Chen, Z. Shi, R. Lawson, P. Sullvian, A. Jen, L. Dalton, and A. Scherer, Nature Mater. **5**, 703 (2006).

⁸S. Noda, M. Fujita, and T. Asano, Nat. Photonics 1, 449 (2007).

⁹S. Combrié, N. Tran, A. De Rossi, and H. Benisty, Opt. Lett. **33**, 1908 (2008).

¹⁰M. Soljačić and J. D. Joannopoulos, Nature Mater. 3, 211 (2004).

¹¹X. Yang and C. W. Wong, Opt. Express **15**, 4763 (2007).

¹²T. J. Johnson, M. Borselli, and O. Painter, Opt. Express 14, 817 (2006).

¹³E. Weidner, S. Combrié, A. De Rossi, N. V. Quynh, and S. Cassette, Appl. Phys. Lett. **90**, 101118 (2007).

¹⁴A. Bristow, J.-P. R. Wells, W. H. Fan, A. M. Fox, M. S. Skolnick, D. M. Whittaker, A. Tahraoui, T. F. Krauss, and J. S. Roberts, Appl. Phys. Lett. 83, 851 (2003).

¹⁵K. Nozaki, H. Watanabe, and T. Baba, Appl. Phys. Lett. **92**, 021108 (2008).

¹⁶A. Yacomotti, F. Raineri, G. Vecchi, P. Monnier, R. Raj, A. Levenson, B. Ben Bakir, X. Seassal, C. Letartre, P. Viktorovitch, L. Di Cioccio, and J. M. Fedeli, Appl. Phys. Lett. 88, 231107 (2006).

¹⁷S. Combrié, S. Bansropun, M. Lecomte, O. Parillaud, S. Cassette, H. Benisty, and J. Nagle, J. Vac. Sci. Technol. B 23, 1521 (2005).

¹⁸S. Combrié, E. Weidner, A. De Rossi, S. Bansropun, S. Cassette, A. Talneau, and H. Benisty, Opt. Express 14, 7353 (2006).

¹⁹T. Liang, H. Tsang, I. Day, J. Drake, A. Knights, and M. Ashari, Appl. Phys. Lett. **81**, 1323 (2002).

²⁰S. Combrié, A. De Rossi, L. Morvan, S. Tonda, S. Cassette, D. Dolfi, and A. Talneau, Electron. Lett. **42**, 86 (2006).

²¹A. De Rossi, M. Lauritano, S. Combrié, Q. Tranh, and C. Husko, arXiv:0812.2058 (unpublished).